Journal of Cardiovascular Computed Tomography 13 (2019) 134–141

Contents lists available at ScienceDirect

Journal of Cardiovascular Computed Tomography

journal homepage: www.elsevier.com/locate/jcct

# Optimized interpretation of fractional flow reserve derived from computed tomography: Comparison of three interpretation methods

Hidenobu Takagi[a,*], Yu Ishikawa[b], Makoto Orii[a], Hideki Ota[c], Masanobu Niiyama[b], Ryoichi Tanaka[a], Yoshihiro Morino[b], Kunihiro Yoshioka[a]

[a] Department of Radiology, Iwate Medical University, 19-1, Uchimaru, Morioka, #0208505, Japan
[b] Division of Cardiology, Department of Internal Medicine, Iwate Medical University, 19-1, Uchimaru, Morioka, #0208505, Japan
[c] Department of Diagnostic Radiology, Tohoku University, 1-1, Seiryo, Sendai, Miyagi, #9808574, Japan

ARTICLE INFO

*Keywords:*
Coronary artery disease
Fractional flow reserve
Coronary computed tomography angiography
Fractional flow reserve derived from computed tomography

ABSTRACT

*Background:* An optimal system for interpreting fractional flow reserve (FFR) values derived from CT ($FFR_{CT}$) is lacking. We sought to evaluate performance of three $FFR_{CT}$ measurements in detecting ischemia by comparing them with invasive FFR.

*Methods:* For 73 vessels in 50 patients who underwent coronary CT angiography (CCTA) and $FFR_{CT}$ analysis followed by invasive FFR, the greatest diameter stenosis on CCTA, $FFR_{CT}$ difference between distal and proximal to the stenosis ($\Delta FFR_{CT}$), $FFR_{CT}$ 2 cm distal to the stenosis (lesion-specific $FFR_{CT}$), and the lowest $FFR_{CT}$ in distal vessel tip were calculated. Significant obstruction ($\geq$50% diameter stenosis) and ischemia (lesion-specific $FFR_{CT}$ $\leq$0.80, the lowest $FFR_{CT}$ $\leq$0.80, or $\Delta FFR_{CT}$ $\geq$0.12 based on the greatest Youden index) were compared with invasive FFR ($\leq$0.80).

*Results:* Forty (55%) vessels demonstrated ischemia during invasive FFR. On multivariable generalized estimating equations, $\Delta FFR_{CT}$ (odds ratio [OR] 10.2, $p < 0.01$) remained a predictor of ischemia over CCTA (OR 2.9), lesion-specific $FFR_{CT}$ (OR 3.1), and the lowest $FFR_{CT}$ (OR 0.9) ($p > 0.05$ for all). Area under the curve (AUC) of $\Delta FFR_{CT}$ (0.86) was higher than CCTA (0.66), lesion-specific $FFR_{CT}$ (0.71), and the lowest $FFR_{CT}$ (0.65) ($p < 0.01$ for all). Addition of each $FFR_{CT}$ measure to CCTA showed improvement of AUC and significant net reclassification improvement (NRI): $\Delta FFR_{CT}$ (AUC 0.84, NRI 1.24); lesion-specific $FFR_{CT}$ (AUC 0.77, NRI 0.83); and the lowest $FFR_{CT}$ (AUC 0.76, NRI 0.59) ($p < 0.01$ for all).

*Conclusions:* Compared with diameter stenosis, $\Delta FFR_{CT}$, lesion-specific $FFR_{CT}$, and the lowest $FFR_{CT}$ improved ischemia discrimination and reclassification, with $\Delta FFR_{CT}$ being superior in identifying and discriminating ischemia.

## 1. Introduction

Fractional flow reserve (FFR) is currently considered as the gold standard for the assessment of ischemia and guides the revascularization in patients with stable coronary artery disease.[1,2] The application of computational fluid dynamics to coronary computed tomography angiography (CCTA) enables noninvasive FFR measurement without hyperemia, which provides information on FFR along the entire coronary artery based on CCTA data sets.[3] Recently, large accuracy and clinical utility studies have validated the FFR derived from CCTA ($FFR_{CT}$).[4–8]

However, in the clinical setting, it is uncertain how physicians should interpret the $FFR_{CT}$ results. In the accuracy trials, diagnostic performance has been determined through a comparison of single measurements at specified locations within the coronary artery corresponding to the location of FFR pressure wire sensor between $FFR_{CT}$ and invasive FFR.[4–6] The data set of $FFR_{CT}$ can provide FFR values along the entire course of the epicardial coronary arteries. Due to a gradual decrease in the $FFR_{CT}$ value even without a focal stenosis, different measurement locations for $FFR_{CT}$ and invasive FFR will produce a different diagnosis, if the respective values are discordant regarding the defined threshold for ischemia of 0.80. Invasive coronary angiography (ICA) and FFR are generally downstream tests of CCTA and $FFR_{CT}$ analyses. Thus, when physicians interpret $FFR_{CT}$ results, they

* Corresponding author. Department of Radiology, Iwate Medical University, 19-1, Uchimaru, Morioka, Iwate, #0208505, Japan.
*E-mail addresses:* hdnb69tkg@gmail.com (H. Takagi), y.ishi@wonder.ocn.ne.jp (Y. Ishikawa), kori931@gmail.com (M. Orii), h-ota@rad.med.tohoku.ac.jp (H. Ota), dekohokuro0516@gmail.com (M. Niiyama), rtanaka@iwate-med.ac.jp (R. Tanaka), ymorino@smile.email.ne.jp (Y. Morino), kyoshi@iwate-med.ac.jp (K. Yoshioka).

https://doi.org/10.1016/j.jcct.2018.10.027
Received 8 June 2018; Received in revised form 29 September 2018; Accepted 24 October 2018
Available online 25 October 2018

**Abbreviations**

| | |
|---|---|
| AUC | area under the curve |
| CI | confidence interval |
| CCTA | coronary computed tomography angiography |
| FFR | fractional flow reserve |
| $FFR_{CT}$ | fractional flow reserve derived from coronary computed tomography angiography |
| ICA | invasive coronary angiography |
| NPV | negative predictive value |
| PPV | positive predictive value |
| ROC | receiver operating characteristics |

cannot apply the position where invasive FFR is measured to $FFR_{CT}$, and reported $FFR_{CT}$ values may not reflect the precise location of the FFR pressure wire sensor. Therefore, an interpretation method for $FFR_{CT}$ results is required in the clinical setting. The lowest $FFR_{CT}$ is the value at the distal end of the coronary vessel, which is commonly used in clinical trials.[9–11] Kueh reported that lesion-specific $FFR_{CT}$, defined as the value within 2 cm distal to the greatest stenotic lesion, could effectively reclassify the positive result in the lowest $FFR_{CT}$.[12]

During invasive FFR, a pullback of the pressure wire is usually performed, with the jump-up of coronary pressure and FFR across the stenosis observed. If coronary stenosis is more severe, pressure gradient across the stenosis becomes higher. Thus, considering pressure gradients across the hemodynamically significant stenosis, we hypothesized that a difference of $FFR_{CT}$ value between distal and proximal to an anatomical stenosis with the greatest diameter stenosis ($\Delta FFR_{CT}$) could become a predictor for ischemia. In this study, we investigated discrimination power, diagnostic performance, and reclassification ability of $\Delta FFR_{CT}$, lesion-specific $FFR_{CT}$, and the lowest $FFR_{CT}$ for the detection of ischemia compared with invasive FFR as the reference standard.

## 2. Methods

### 2.1. Study design and population

This retrospective single-center study was approved by an institutional review board, and included patients from a prospective registry assessing the diagnostic value of noninvasive $FFR_{CT}$ in coronary care (ADVANCE registry, ClinicalTrials.gov #NCT02499679).[13] We obtained written informed consent for the registry from all participants, and the institutional review board waived the requirement of additional informed consent for this sub-analyses. Table S1 (supplementary material) provides inclusion and exclusion criteria for the registry. Consecutive participants in the prospective registry who underwent CCTA with $FFR_{CT}$ analysis followed by invasive FFR measurement in our institution between September 2015 and September 2017 were included. Patients were excluded if they had prior coronary artery bypass graft surgery or percutaneous coronary intervention.

### 2.2. CT acquisition and interpretation

All patients underwent coronary CT calcium scoring and angiography,[14] using the following CT scanners: 0.5 mm × 320-row detector CT scanner (Aquilion ONE ViSION or Genesis Edition, Canon Medical Systems, Otawara, Japan), 0.25 mm × 128-row (TSX-304R, Canon Medical Systems) or 0.25 mm × 160-row (Aquilion Precision, Canon Medical Systems) ultra-high-resolution CT scanner.[15] Patient preparation and CT scanning were performed based on the Society of Cardiovascular Computed Tomography (SCCT) guidelines.[16,17] All patients took nitroglycerin. Patients with a heart rate of 65 beats/min received intravenous beta-blockers 5–7 min before CCTA scan. All CCTA procedures were performed with a prospective electrocardiogram-gated scan. The detailed CCTA protocol is summarized in Table S2 (supplementary material). The optimal stationary cardiac phase with minimum motion-free datasets was determined by cardiovascular CT technologists. Both the volumetric CT dose index and dose-length product were recorded for each patient. The corresponding effective radiation dose was calculated using a conversion factor of 0.014 mSv/mGy cm.[18] Coronary stenosis severity was assessed by radiologists with more than 20 years experience (RT and KY) using a commercially available workstation (Ziostation2, Ziosoft, Tokyo, Japan). The degree of coronary stenosis was graded as minimal (< 25%), mild (25%–49%), moderate (50%–69%), and severe (70%–99%) according to the SCCT guideline.[19] Significant obstruction was defined as luminal stenosis of ≥ 50%.

### 2.3. $FFR_{CT}$ analysis

$FFR_{CT}$ analysis was blindedly and independently performed at HeartFlow Inc., Redwood City, CA, USA. The results provide $FFR_{CT}$ value throughout the coronary arterial tree. For each coronary artery, a radiologist (HT with 7 years experience) calculated three parameters as

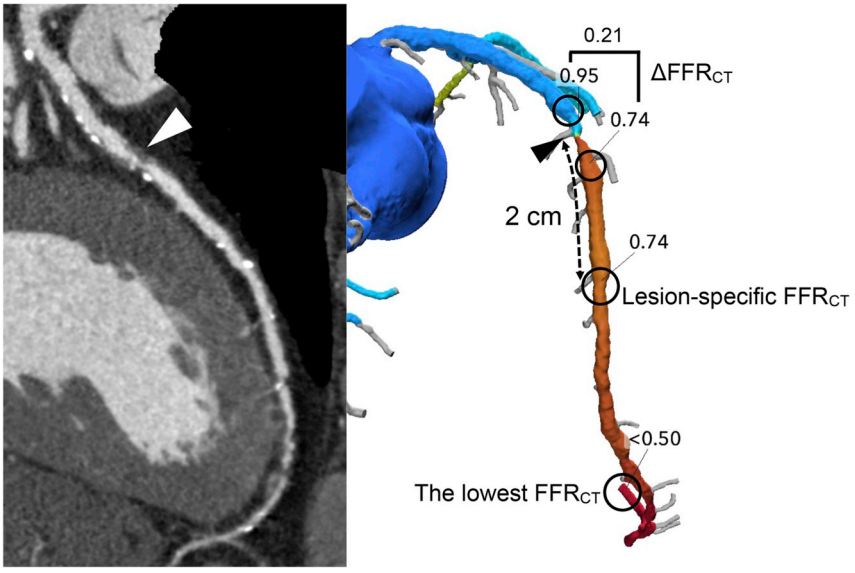


**Fig. 1.** Quantitative parameters derived from $FFR_{CT}$.
$\Delta FFR_{CT}$ was calculated as the difference of values in proximal and distal sites, which were manually selected to be the most adjacent points to the maximal stenosis in which there was minimal or no plaque. Lesion-specific $FFR_{CT}$ was defined as the value at 2 cm distal to the maximal stenosis. The lowest $FFR_{CT}$ was the value at the distal end of the coronary vessel in $FFR_{CT}$.
$FFR_{CT}$ = fractional flow reserve derived from computed tomography.

follows: a difference of $FFR_{CT}$ values between distal and proximal to an anatomical stenosis with greatest stenosis on the coronary vessel ($\Delta FFR_{CT}$), $FFR_{CT}$ value within 2 cm distal to the tightest point (lesion-specific $FFR_{CT}$), and the lowest $FFR_{CT}$ value in the distal vessel tip (the lowest $FFR_{CT}$) (Fig. 1). Fig. 2 shows a detailed method on how to obtain the $\Delta FFR_{CT}$. For lesion-specific $FFR_{CT}$, the tightest point similar to that employed in $\Delta FFR_{CT}$ was used, and the position 2 cm distal to the location was measured on a curved planar reconstructed image. When serial lesions were observed, only the lesion with greatest diameter stenosis was used, and the value was measured strictly at 2 cm distal to the tightest point regardless of the presence or absence of plaque. If lesion-specific $FFR_{CT}$ was distal to the distal vessel tip on $FFR_{CT}$, values in the distal tip were employed as the lesion-specific $FFR_{CT}$ (i.e. lesion-specific $FFR_{CT}$ = the lowest $FFR_{CT}$). Given that $FFR_{CT}$ does not provide a value of less than 0.50, the value of < 0.50 was defined as 0.50. Ischemia was defined as an $FFR_{CT}$ value of ≤0.80 for lesion-specific $FFR_{CT}$ and the lowest $FFR_{CT}$. To assess interobserver reproducibility, another radiologist (MO with 10 years experience) independently and blindly calculated these $FFR_{CT}$ measures for consecutive 30 vessels. The optimal threshold value of $\Delta FFR_{CT}$ was defined as values corresponding to the maximum Youden index in the receiver operating characteristic (ROC) curve.[20]

### 2.4. ICA and FFR measurements

Cardiologists performed ICA and FFR on a biplane angiography system. FFR was performed with a 0.014-inch pressure monitoring wire (PressureWire Aeris, St. Jude Medical Systems, USA). Hyperemia was attained after administration of intravenous adenosine triphosphate (140 μg/kg/min, n = 37) or intracoronary nicorandil (2 mg, n = 13). FFR was calculated automatically by dividing the mean distal coronary pressure by the mean aortic pressure during hyperemia. The position of the distal pressure sensor was recorded, and compared with 2 cm distal to the tightest point (i.e. position of lesion-specific $FFR_{CT}$) and the distal end of $FFR_{CT}$ (i.e. position of the lowest $FFR_{CT}$) (Fig. 3). FFR was considered diagnostic of ischemia at a threshold of ≤0.80.

### 2.5. Statistical analysis

No power analysis was performed because of the lack of previous studies on the topic. Descriptive statistics were presented as mean ± standard deviation (SD) for normally distributed variables (Shapiro-Wilk test, $p \geq 0.05$), as medians with interquartile ranges for non-normally distributed variables, and as numbers of cases (and percentages) per group for categorical variables. The interobserver reproducibilities were assessed using intraclass correlation coefficients (ICC) for absolute agreement of single measures with 95% confidence interval (CI). The per-vessel area under the curve (AUC), accuracy, sensitivity, specificity, and positive predictive (PPV) and negative predictive value (NPV) for the detection of ischemia compared with invasive FFR were calculated with 95% CI. AUC comparisons were performed as previously described by DeLong.[21] Comparisons of accuracy, sensitivity, and specificity were performed by using the Cochran's Q tests, followed by between-group comparisons using post-hoc Dunn's tests with Bonferroni correction.[22] Bootstrapping with 10,000 samples was used for adjustment for clustering effects in the 95% CI, and for comparison of diagnostic performance. Binary logistic generalized estimating equations were used to evaluate the relationship between $FFR_{CT}$ parameters and ischemia determined by invasive FFR, since multiple vessels per patient were counted. Additive values of each $FFR_{CT}$ measure was evaluated by category-free net reclassification improvement (NRI).[23,24] Computations were performed using JMP Pro 12.2 (SAS Institute Inc., Cary, NC, USA), SPSS Statistics version 25 (IBM corporation, Armonk, NY, USA) or R 3.3.3 (R Foundation for Statistical Computing, Vienna, Austria) software. Two-sided $p < 0.05$ indicated statistical significance.

## 3. Results

### 3.1. Study population and characteristics

Among 106 patients who underwent $FFR_{CT}$ analysis, forty-one (39%) patients defer ICA based on CCTA/$FFR_{CT}$ results. Fourteen patients who underwent ICA without invasive FFR measurement and one patient with history of PCI were excluded. Consequently, this study included 73 vessels with > 25% stenosis in 50 patients (1.5 vessels per patient) (Fig. 4). Patient and CCTA characteristics are summarized in Tables 1 and 2, respectively. Ischemia was found in 55% (40/73) of vessels of 66% (33/50) patients during invasive FFR; mean invasive FFR value was 0.76 ± 0.17. Table 3 provides details on the extent of coronary stenosis. For invasive FFR measurements, five positions of distal wire sensor were missing. In the remaining 68 vessels, the positional relationships of distal pressure sensor to measurement points for lesion-specific $FFR_{CT}$ and the lowest $FFR_{CT}$ were as follows: proximal, 10% (7/68) and 63% (43/68); distal, 60% (41/68) and 13% (9/68); and same position, 29% (20/68) and 24% (16/68), respectively (Fig. 3).

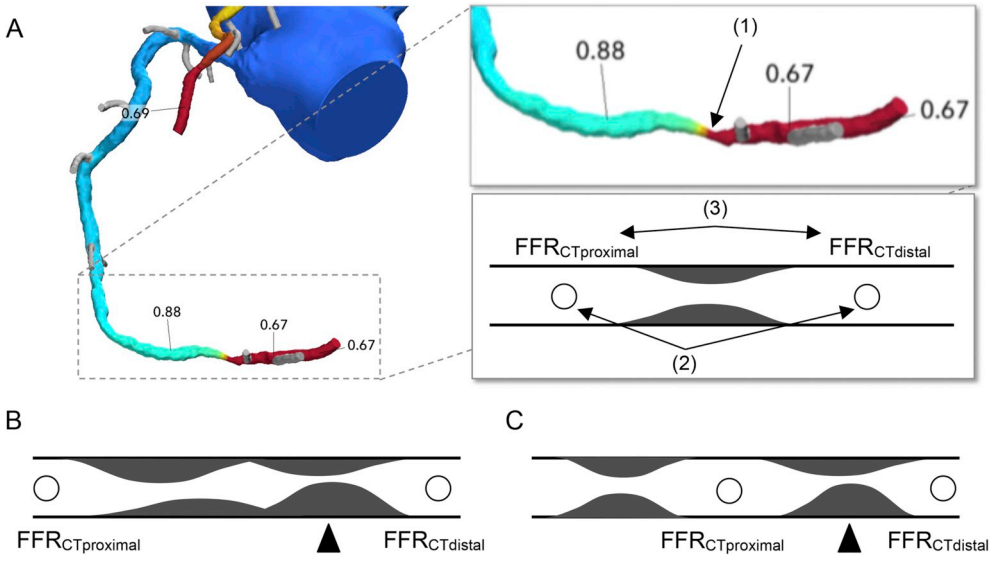


**Fig. 2.** Detailed methods in obtaining $\Delta FFR_{CT}$.
We obtained $\Delta FFR_{CT}$ using the following 3 steps (A): (1) we identified the greatest stenosis in the coronary tree; (2) selected proximal and distal adjacent points to the tightest point in which there is minimal or no plaque; (3) and subtracted $FFR_{CTdistal}$ from $FFR_{CTproximal}$, where $FFR_{CTproximal}$ and $FFR_{CTdistal}$ were defined as $FFR_{CT}$ values at the proximal and distal points, respectively. If there was a diffuse plaque (B), we selected the proximal or distal points for $\Delta FFR_{CT}$ far from the tightest point (arrow head), and the distance between proximal or distal points became longer. In a case with serial lesions (C), we strictly selected proximal and distal points adjacent to the tightest point (arrow head) in which there is minimal or no plaque, independently of other stenosis severity.
$FFR_{CT}$ = fractional flow reserve derived from computed tomography.

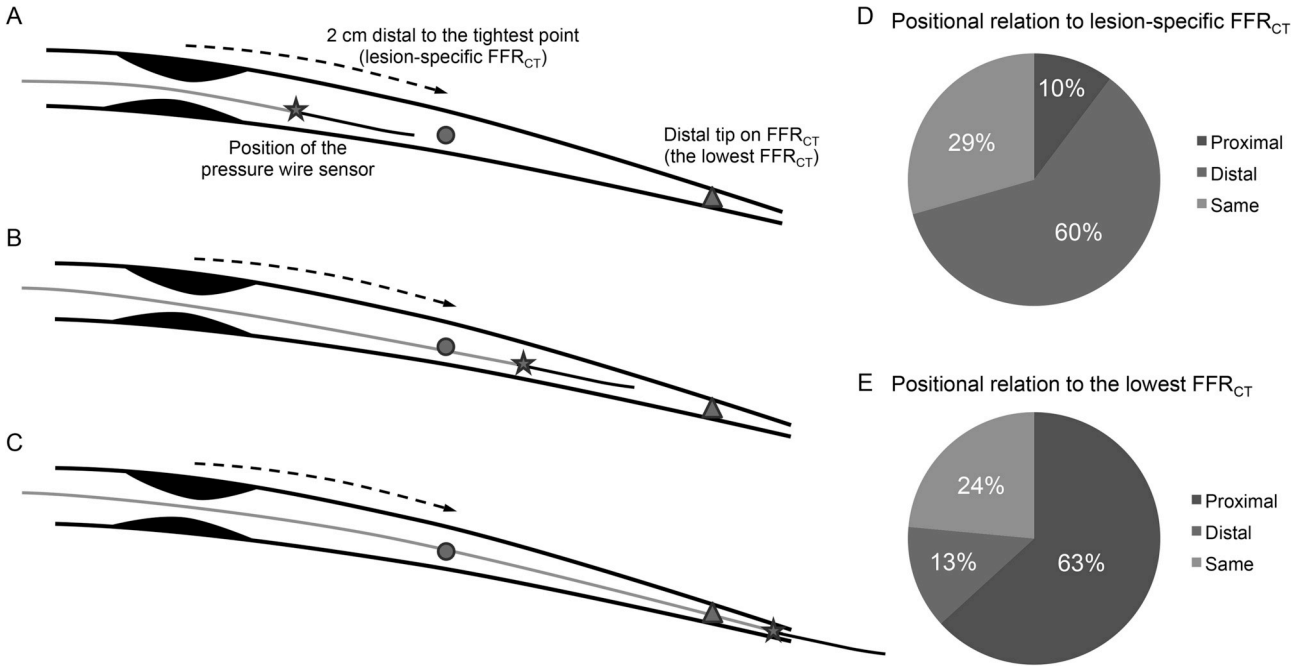


**Fig. 3.** Positional relationship of the pressure wire sensor to the lesion-specific $FFR_{CT}$ and the lowest $FFR_{CT}$.
The position of the distal pressure sensor (star) was compared with the position 2 cm distal to the tightest point (i.e. position of lesion-specific $FFR_{CT}$) (circle) or that at the distal end of $FFR_{CT}$ (i.e. position of the lowest $FFR_{CT}$) (triangle). A shows a pressure sensor positioned proximal to the lesion-specific $FFR_{CT}$ and the lowest $FFR_{CT}$, whereas B and C show a sensor positioned between lesion-specific $FFR_{CT}$ and the lowest $FFR_{CT}$, and distal to both, respectively. In our study, five positions of distal wire sensor were missing. In the remaining 68 vessels, the positional relationships of distal pressure sensor to measurement points for lesion-specific $FFR_{CT}$ (D) and the lowest $FFR_{CT}$ (E) were as follows: proximal, 10% (7/68) and 63% (43/68); distal, 60% (41/68) and 13% (9/68); and same position, 29% (20/68) and 24% (16/68), respectively.
$FFR_{CT}$ = fractional flow reserve derived from computed tomography.

### 3.2. Discrimination of ischemia

Per-vessel AUC for CCTA, $\Delta FFR_{CT}$, lesion-specific $FFR_{CT}$, and the lowest $FFR_{CT}$ were 0.66 (95% CI, 0.56–0.76), 0.86 (95% CI, 0.75–0.92), 0.71 (95% CI, 0.59–0.80), and 0.65 (95% CI, 0.55–0.74), respectively (Fig. 5 A). The optimal threshold value for $\Delta FFR_{CT}$ was 0.12 based on the greatest Youden index. Table 4 provides measures of diagnostic characteristics. The AUC for $\Delta FFR_{CT}$ was higher than all the other parameters: differences in AUC for CCTA, 0.20 (95% CI, 0.09–0.30, $p < 0.01$), lesion-specific $FFR_{CT}$, 0.15 (95% CI, 0.05–0.26, $p < 0.01$), and the lowest $FFR_{CT}$, 0.21 (95% CI, 0.11–0.31, $p < 0.01$), respectively (Fig. 5 A). The specificity for $\Delta FFR_{CT}$ with threshold value of 0.12 was higher than those for CCTA and the lowest $FFR_{CT}$ (adjusted $p < 0.01$ for both). The accuracy and sensitivity showed no statistical significance between CCTA, $\Delta FFR_{CT}$, lesion-specific $FFR_{CT}$ and, the lowest $FFR_{CT}$ (accuracy, $p = 0.126$; and sensitivity, $p = 0.059$, respectively by Cochran's Q test). Fig. 6 displays a representative case of patients with a

**Table 1**
Patient characteristics (N = 50).

| Variables | Values |
|---|---|
| Sex (woman)[a] | 14 (7/50) |
| Age (years) | 71 (57–75) |
| Height (cm) | 164 (160–172) |
| Weight (kg) | 67 (60–75) |
| Body mass index (kg/m$^2$) | 26 (23–27) |
| Hypertension[a] | 74 (37/50) |
| Diabetes[a] | 34 (17/50) |
| Dyslipidemia[a] | 62 (31/50) |
| Current/past smoker[a] | 50 (25/50) |
| Serum creatinine (mg/dl) | 0.82 (0.74–0.90) |
| Estimated glomerular filtration rate (ml/min/1.73m$^2$) | 70 (62–78) |

Note – Unless otherwise noted, data are medians, with quartiles in parentheses.
[a] Data are percentages, with raw data in parentheses.

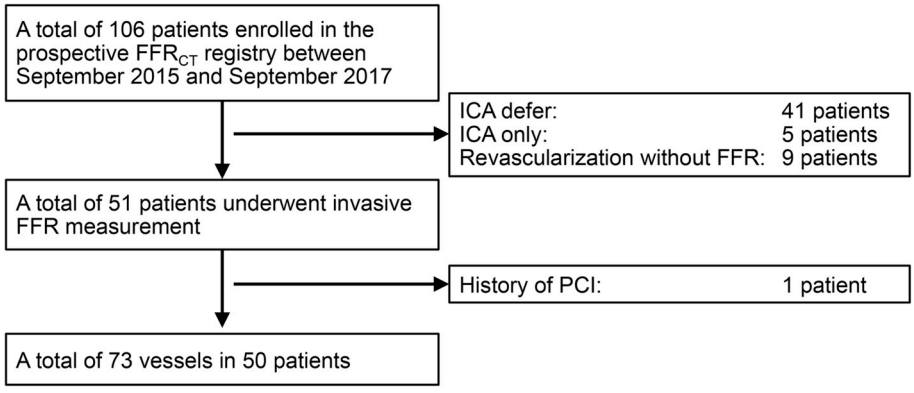


**Fig. 4.** Study enrollment.
Among 106 patients who underwent $FFR_{CT}$ analysis, forty-one (39%) patients defer ICA based on CCTA and $FFR_{CT}$ results. The other fourteen (13%) patients underwent ICA or revascularization without invasive FFR measurement. Consequently, fifty-one patients underwent invasive FFR. One patient with history of PCI was excluded. A total of 73 vessels in 50 patients were analyzed.
$FFR_{CT}$ = fractional flow reserve derived from computed tomography, ICA = invasive coronary angiography, FFR = fractional flow reserve, and PCI = percutaneous coronary intervention.

**Table 2**
CT characteristics (N = 50).

| Variables | Values |
|---|---|
| CT scanner | |
| 0.5 mm × 320-row CT (Aquilion One ViSION) | 24 (12/50) |
| 0.5 mm × 320-row CT (Aquilion One GENESIS) | 26 (13/50) |
| 0.25 mm × 128-row CT (TSX-304R) | 44 (22/50) |
| 0.25 mm × 160-row CT (Aquilion Precision) | 6 (3/50) |
| Agatston score[14a] | 251 (51–531) |
| 0–400 | 62 (31/50) |
| > 400 | 38 (19/50) |
| Nitrate administrated | 100 (50/50) |
| Beta-blocker administrated | 48 (24/50) |
| Arrhythmia | 2 (1/50) |
| Mean heart rate during CCTA (beats per minute)[a] | 57 (52–61) |
| Dose of iodine contrast medium (ml)[a] | 57 (45–67) |
| Volumetric CT dose index for CCTA (mGy)[a] | 23 (9–31) |
| Dose-length product for CCTA (mGy·cm)[a] | 329 (111–449) |
| Effective radiation dose for CCTA (mSv)[ab] | 4.6 (1.6–6.3) |

Note – Unless otherwise noted, data are percentages, with raw data in parentheses.
CCTA = coronary computed tomography angiography.
[a] Data are medians, with quartiles in parentheses.
[b] Effective radiation dose was calculated using a conversion factor of 0.014 mSv/mGy·cm.[18].

**Table 3**
Extent of coronary stenosis (N = 50 patients; N = 73 vessels).

| Variables | Values |
|---|---|
| Vessel with CCTA maximum stenosis of 25–49% | 22 (16/73) |
| Vessel with CCTA maximum stenosis of 50–69% | 51 (37/73) |
| Vessel with CCTA maximum stenosis of 70–99% | 27 (20/73) |
| Patients with CAD-RADS 3[a] | 38 (19/50) |
| Patients with CAD-RADS 4A[a] | 52 (26/50) |
| Patients with CAD-RADS 4B[a] | 6 (3/50) |
| Patients with CAD-RADS 5[a] | 4 (2/50) |
| Vessel with FFR ≤0.80 | 55 (40/73) |
| RCA with FFR ≤0.80 | 57 (8/14) |
| LAD with FFR ≤0.80 | 61 (25/41) |
| LCX with FFR ≤0.80 | 35 (6/17) |
| Patients with FFR ≤0.80 in > 1 vessel | 66 (33/50) |

Note – Data are percentages, with raw data in parentheses.
CCTA = coronary computed tomography angiography, FFR = fractional flow reserve, RCA = right coronary artery, LAD = left anterior descending artery, and LCX = left circumflex.
[a] All patients were graded using Coronary Artery Disease: Reporting and Data System (CAD-RADS) as previously described.[25].

positive result for the lowest $FFR_{CT}$ without ischemia for the invasive FFR.

### 3.3. Diagnosis of ischemia

On univariable generalized estimating equations, CCTA ($X^2$, 6.8, odds radio [OR], 8.0 [95% CI, 1.7–38.4], $p < 0.01$), $\Delta FFR_{CT}$ ($X^2$, 21.2, OR, 18.0 [95% CI, 5.3–61.2], $p < 0.01$), lesion-specific $FFR_{CT}$ ($X^2$, 10.6, OR, 6.0 [95% CI, 2.0–17.8], $p < 0.01$), and the lowest $FFR_{CT}$ ($X^2$, 7.7, OR, 5.9 [95% CI, 1.8–20.4], $p = 0.018$) were related to the ischemia determined by invasive FFR (Table S3, supplementary material). On multivariable generalized estimating equation, $\Delta FFR_{CT}$ ($X^2$, 12.3, OR, 10.2 [95% CI, 2.8–37.3], $p < 0.01$) remained a predictor over CCTA ($X^2$, 1.1, OR, 2.9 [95% CI, 0.4–21.8], $p = 0.30$), lesion-specific $FFR_{CT}$, ($X^2$, 2.9, OR, 3.1 [95% CI, 0.8–11.1], $p = 0.091$), and the lowest $FFR_{CT}$ ($X^2$, 0.01, OR, 0.9 [95% CI, 0.2–5.1], $p = 0.95$) (Table S3, supplementary material).

### 3.4. Additive values of $FFR_{CT}$ parameters

All diagnostic models using CCTA and $FFR_{CT}$ measures demonstrated higher AUC than the model with CCTA alone (CCTA alone, 0.66 [95% CI, 0.56–0.75]; CCTA + $\Delta FFR_{CT}$, 0.84 [95% CI, 0.73–0.91]; CCTA + lesion-specific $FFR_{CT}$, 0.77 [95% CI, 0.65–0.86]; and CCTA + the lowest $FFR_{CT}$, 076 [95% CI, 0.65–0.85], $p < 0.01$ for all) (Fig. 5 B, C, and D). All $FFR_{CT}$ parameters enabled effective reclassification of CCTA diameter stenosis as follows: $\Delta FFR_{CT}$ (NRI, 1.24 [95% CI, 0.87–1.60], $p < 0.01$); lesion-specific $FFR_{CT}$ (NRI, 0.83 [95% CI, 0.40–1.25], $p < 0.01$); and the lowest $FFR_{CT}$ (NRI, 0.59 [95% CI, 0.21–0.97], $p < 0.01$).

### 3.5. Relationship between $FFR_{CT}$ parameters and stenosis grading

The relationships between $FFR_{CT}$ measures and anatomical stenosis determined by CCTA are displayed in Fig. 7. All 20 vessels with severe (70%–99%) stenosis demonstrated hemodynamic significance on invasive FFR. Vessels with mild (25%–49%) and moderate (50%–69%) stenoses included 19% (3/16) and 46% (17/37), respectively, of vessels with ischemia. For the 37 moderate stenotic lesions, $\Delta FFR_{CT}$, lesion-specific $FFR_{CT}$ and the lowest $FFR_{CT}$ correctly reclassified 43% (16/37), 32% (12/37), and 24% (9/37), respectively, of vessels into the non-ischemia (invasive FFR > 0.80). For the remaining 16 vessels with mild stenotic lesions, $\Delta FFR_{CT}$ could not reclassify into the ischemia (invasive FFR ≤0.80), while lesion-specific $FFR_{CT}$, and the lowest $FFR_{CT}$ correctly reclassified 13% (2/16) and 13% (2/16) of vessels, respectively into the ischemia (invasive FFR ≤0.80).

### 3.6. Interobserver reproducibility

For each $FFR_{CT}$ measures, intraclass correlation coefficients were as follows: $\Delta FFR_{CT}$, 0.90 (95% CI, 0.79–0.95); lesion-specific $FFR_{CT}$, 0.86 (95% CI, 0.73–0.93); and the lowest $FFR_{CT}$, 1.00 (95% CI, 0.99–1.00).

## 4. Discussion

At present, interpreting or reporting $FFR_{CT}$ result system in a clinical condition is lacking. We developed $\Delta FFR_{CT}$ as a predictor of ischemia, and investigated discrimination power, diagnostic accuracy and reclassification ability of $\Delta FFR_{CT}$, lesion-specific $FFR_{CT}$, and the lowest $FFR_{CT}$. Each $FFR_{CT}$ measure showed improvement of AUC and effective reclassifications for the detection of ischemia, compared with those of CCTA alone. Among these $FFR_{CT}$ measures, $\Delta FFR_{CT}$ showed the highest AUC, and the specificity of $\Delta FFR_{CT}$ with threshold value of 0.12 was higher compared to that of the lowest $FFR_{CT}$. The per-vessel sensitivity and specificity of $\Delta FFR_{CT}$ were comparable to those in the NXT trial (sensitivity and specificity of 84% and 86%, respectively).[6] Multivariable generalized estimating equation showed that $\Delta FFR_{CT}$ remained a predictor of ischemia over CCTA, lesion-specific $FFR_{CT}$, and the lowest $FFR_{CT}$. Furthermore, these $FFR_{CT}$ measures could efficiently reclassify moderate stenotic lesions and be limited to vessels with mild or severe stenosis. Combined with anatomical stenosis evaluation, $\Delta FFR_{CT}$, lesion-specific $FFR_{CT}$, and the lowest $FFR_{CT}$ will aid in the diagnosis of ischemia. Moreover, from the perspective of clinical use, the advantage of these parameters is that the measurement is not based on the position of the pressure wire sensor. Thus, these $FFR_{CT}$ measurements, which are intended for clinical use, will enhance the clinical value of $FFR_{CT}$ when managing patients with suspected ischemia.

However, in our study, more than half (63%) of invasive FFR measurements were performed proximal to the lowest $FFR_{CT}$, whereas 60% were performed distal to the lesion-specific $FFR_{CT}$. Considering that there is a gradual decrease in the $FFR_{CT}$ value even without a focal stenosis, positional differences could cause discordances in values between $FFR_{CT}$ and invasive FFR. If the same threshold value of 0.80 for ischemia is used, the lowest $FFR_{CT}$ could overestimate the severity of

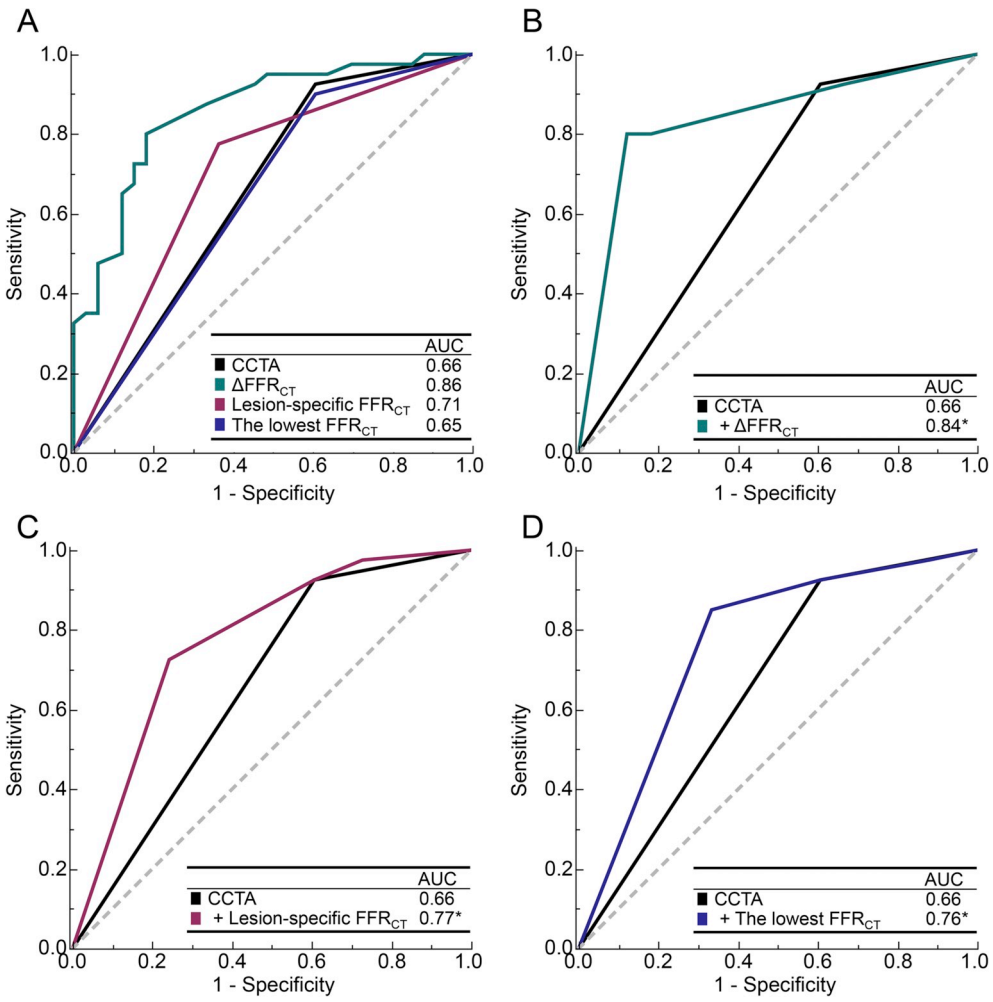


**Fig. 5.** Receiver operating characteristic (ROC) curves of CCTA, $\Delta FFR_{CT}$, lesion-specific $FFR_{CT}$, and the lowest $FFR_{CT}$ in predicting ischemia (N = 73 vessels).
A shows ROC curves for predicting ischemia using CCTA, $\Delta FFR_{CT}$, lesion-specific $FFR_{CT}$, and the lowest $FFR_{CT}$. B, C and D show the ROC curves of models using CCTA with and without $\Delta FFR_{CT}$, lesion-specific $FFR_{CT}$, and the lowest $FFR_{CT}$, respectively. Threshold value of 0.12 corresponding to the maximum Youden index was used for the comparison between CCTA and CCTA with $\Delta FFR_{CT}$.
*Indicates statistically significant difference between AUC for CCTA and CCTA with parameters derived from $FFR_{CT}$ (B, C, and D) using DeLong test.[21]
CCTA = coronary computed tomography angiography, $FFR_{CT}$ = fractional flow reserve derived from computed tomography, and AUC = area under the curve.

**Table 4**
Per-vessel diagnostic accuracy of CCTA, $\Delta FFR_{CT}$, lesion-specific $FFR_{CT}$ and the lowest $FFR_{CT}$ (N = 73).

| Variables | CCTA[b] | $\Delta FFR_{CT}$[c] | Lesion-specific $FFR_{CT}$[d] | The lowest $FFR_{CT}$[d] |
|---|---|---|---|---|
| True positive[a] | 37 | 32 | 31 | 36 |
| True negative[a] | 13 | 27 | 21 | 13 |
| False positive[a] | 20 | 6 | 12 | 20 |
| False negative[a] | 3 | 8 | 9 | 4 |
| % Accuracy | 69 (59–74) | 81 (70–88) | 71 (60–80) | 67 (58–73) |
| % Sensitivity | 93 (84–97) | 80 (71–87) | 78 (68–86) | 90 (81–96) |
| % Specificity | 39 (29–45) | 82 (70–90) | 64 (51–74) | 39 (29–46) |
| % PPV | 65 (59–68) | 84 (74–91) | 72 (63–80) | 64 (58–68) |
| % NPV | 81 (60–93) | 77 (66–85) | 70 (57–81) | 77 (56–90) |
| AUC | 0.66 (0.56–0.76) | 0.86 (0.75–0.92) | 0.71 (0.59–0.80) | 0.65 (0.55–0.74) |

Note – Unless otherwise noted, data are measures, with 95% confidence intervals.
CCTA = coronary computed tomography angiography, $FFR_{CT}$ = fractional flow reserve derived from computed tomography, AUC = area under the curve, NPV = negative predictive value, and PPV = positive predictive value.
[a] Data are raw data.
[b] For CCTA, significant obstruction was defined as diameter stenosis of ≥50%.
[c] For $\Delta FFR_{CT}$, diagnostic characteristics were calculated using the threshold value of 0.12 corresponding to the maximum Youden index.
[d] For lesion-specific $FFR_{CT}$ or the lowest $FFR_{CT}$, functional significant was defined as $FFR_{CT}$ value of ≤0.80.

the lesion compared with invasive FFR, whereas lesion-specific $FFR_{CT}$ could underestimate the severity. Thus, these measurements do not precisely reflect invasive FFR results, and simply reporting the lowest $FFR_{CT}$ or lesion-specific $FFR_{CT}$ alone can confuse rather than help in clinical decision-making when considering referral for ICA. Especially, the AUC (0.65) and specificity (39%) of the lowest $FFR_{CT}$ were modest, which probably account for the disagreement of the measurement location. The lowest $FFR_{CT}$ might have a tendency to become lower than those measured at the proximal to the distal vessel tip. These results indicate that simply using the lowest $FFR_{CT}$ is unreliable, and a system for interpreting $FFR_{CT}$ results should be reconsidered in clinical settings.

Our study has some limitations. It is a single-center study with a small sample size. Moreover, although this study included patients from the prospective registry, this subanalysis is not prespecified. Additionally, the population consisted of patients who underwent invasive ICA and FFR, which causes a potential selection bias of patients referred for $FFR_{CT}$ evaluation and those subsequently referred for ICA and FFR. Patients who had previously undergone revascularization were also excluded from the study. Thus, the usefulness of $FFR_{CT}$ parameters warrants further investigation. Furthermore, this study lacks clinical outcome data, such as reduction of unnecessary ICA or adverse cardiac events. For those reasons, we could just conclude that $\Delta FFR_{CT}$, lesion-specific $FFR_{CT}$, and the lowest $FFR_{CT}$ will help in interpreting $FFR_{CT}$ results in patients referred for ICA and invasive FFR measurement. To show the usefulness of these methods, a further clinical outcome study is needed.

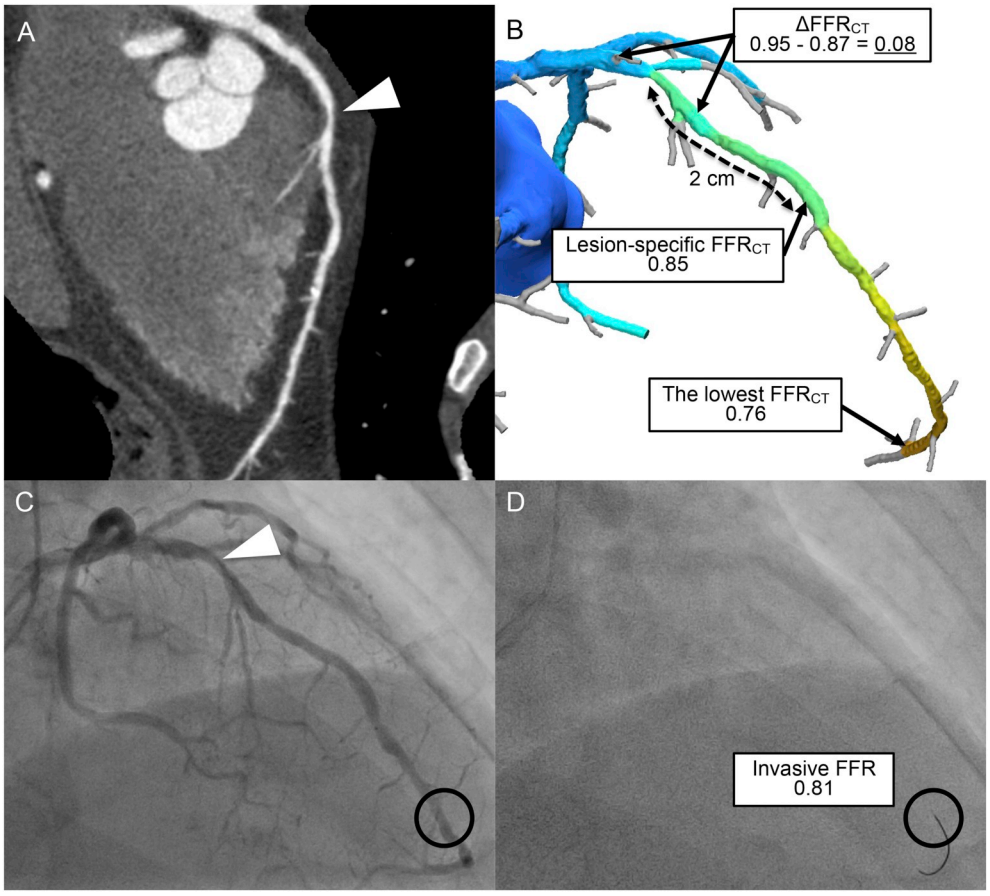


**Fig. 6.** Representative case example from a study.
A 70-year-old man with atypical chest pain. Curved planar reconstruction image of CCTA (A) shows a moderate stenosis (50%–69% diameter stenosis) in the proximal left anterior descending artery (arrow head). Although the lowest $FFR_{CT}$ is 0.76, which suggests ischemia, $\Delta FFR_{CT}$ and lesion-specific $FFR_{CT}$ suggest non-ischemic lesion (B). Invasive FFR measurement was performed at the proximal to the distal vessel tip of $FFR_{CT}$ (circles), in which the value of 0.81 suggests non-ischemia (C and D).
$FFR_{CT}$ = fractional flow reserve derived from computed tomography, and CCTA = coronary computed tomography angiography.

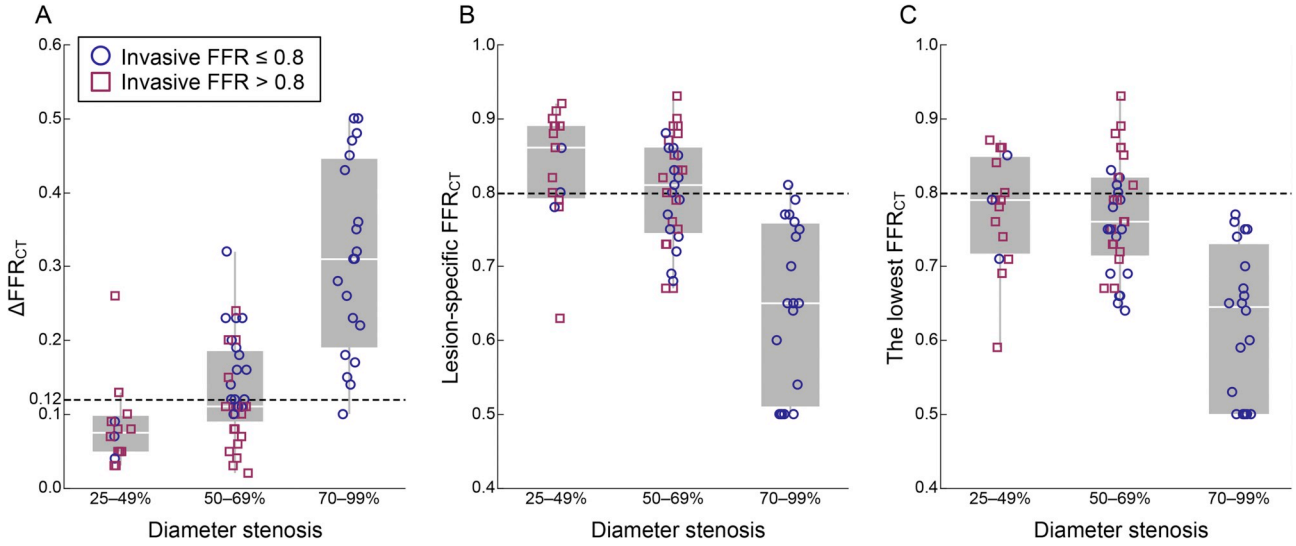


**Fig. 7.** Relationship between $FFR_{CT}$ measures and anatomical stenosis determined by CCTA.
Distributions of $\Delta FFR_{CT}$ (A), lesion-specific $FFR_{CT}$ (B), and the lowest $FFT_{CT}$ (C) in each group with 25%–49%, 50%–69%, and 70%–99% diameter stenosis determined by CCTA are shown. Box and plots show the medians, quartiles, and ranges in $FFR_{CT}$ parameters. Individual values are also shown as a circle (invasive FFR ≤0.80) or a square (invasive FFR > 0.80). Threshold values of each $FFR_{CT}$ parameter are displayed as dashed lines. All 20 vessels with 70%–99% diameter stenosis demonstrated functional significance during invasive FFR, and vessels with 25%–49% or 50%–69% included 19% (3/16) or 54% (20/37) of vessels without ischemia, respectively.
$FFR_{CT}$ = fractional flow reserve derived from computed tomography, and FFR = fractional flow reserve.

## 5. Conclusions

Although $FFR_{CT}$ is a clinically useful diagnostic tool, a standardized interpretation system is lacking in clinical settings. Adding $\Delta FFR_{CT}$, lesion-specific $FFR_{CT}$, and the lowest $FFR_{CT}$ to the diameter stenosis determined by CCTA showed improvements in discriminating and effectively reclassifying ischemia, with $\Delta FFR_{CT}$ being superior in identifying and discriminating ischemia. In contrast, the lowest $FFR_{CT}$ was of

limited value, which suggests that positional difference between $FFR_{CT}$ and invasive FFR may have a potential harm; thus, cautious clinical interpretation of $FFR_{CT}$ values is crucial.

## Funding sources

This work was supported by Grant-in-Aid for Young Scientists (B) from the Japan Society for the Promotion of Science [Grant Number, 17K18044]; and Program for the Private University Research Branding Project from the Ministry of Education, Culture, Sports, Science and Technology. ADVANCE registry was supported by HeartFlow, Inc., Redwood City, CA, USA.

## Disclosure/conflict of interest

The 7th author (YM) is speaker bureau for Abbott Vascular. Other authors declare that they have no conflict of interests.

## Acknowledgement

The authors acknowledge members of the Division of Cardiovascular Radiology and Division of Cardiology for kind support to this study.

## Appendix A. Supplementary data

Supplementary data to this article can be found online at https://doi.org/10.1016/j.jcct.2018.10.027.

## References

1. Fihn SD, Gardin JM, Abrams J, et al. Accf/aha/acp/aats/pcna/scai/sts guideline for the diagnosis and management of patients with stable ischemic heart disease: a report of the American college of Cardiology foundation/American heart association task force on practice guidelines, and the American college of physicians, American Association for thoracic surgery, preventive cardiovascular nurses association, society for cardiovascular angiography and interventions, and society of thoracic surgeons. *Circulation.* 2012;126(25):e354–e471. https://doi.org/10.1161/CIR.0b013e318277d6a0.
2. Windecker S, Kolh P, Alfonso F, et al. ESC/EACTS guidelines on myocardial revascularization: the task force on myocardial revascularization of the European society of Cardiology (ESC) and the European association for cardio-thoracic surgery (EACTS)developed with the special contribution of the European association of percutaneous cardiovascular interventions (EAPCI). *Eur Heart J.* 2014;35(37):2541–2619. https://doi.org/10.1093/eurheartj/ehu278.
3. Taylor CA, Fonte TA, Min JK. Computational fluid dynamics applied to cardiac computed tomography for noninvasive quantification of fractional flow reserve. *J Am Coll Cardiol.* 2013;61(22):2233–2241. https://doi.org/10.1016/j.jacc.2012.11.083.
4. Koo B-K, Erglis A, Doh J-H, et al. Diagnosis of ischemia-causing coronary stenoses by noninvasive fractional flow reserve computed from coronary computed tomographic angiograms: results from the prospective multicenter DISCOVER-FLOW (diagnosis of ischemia-causing stenoses obtained via noninvasive fractional flow reserve) study. *J Am Coll Cardiol.* 2011;58(19):1989–1997. https://doi.org/10.1016/j.jacc.2011.06.066.
5. Min JK, Leipsic J, Pencina MJ, et al. Diagnostic accuracy of fractional flow reserve from anatomic CT angiography. *J Am Med Assoc.* 2012;308(12):1237. https://doi.org/10.1001/2012.jama.11274.
6. Nørgaard BL, Leipsic J, Gaur S, et al. Diagnostic performance of noninvasive fractional flow reserve derived from coronary computed tomography angiography in suspected coronary artery disease. *J Am Coll Cardiol.* 2014;63(12):1145–1155. https://doi.org/10.1016/j.jacc.2013.11.043.
7. Douglas PS, Pontone G, Hlatky MA, et al. Clinical outcomes of fractional flow reserve by computed tomographic angiography-guided diagnostic strategies vs. usual care in patients with suspected coronary artery disease: the prospective longitudinal trial of FFRCT: outcome and resource impacts study. *Eur Heart J.* 2015;36(47):3359–3367. https://doi.org/10.1093/eurheartj/ehv444.
8. Douglas PS, De Bruyne B, Pontone G, et al. 1-Year outcomes of FFRCT-guided care in patients with suspected coronary disease. *J Am Coll Cardiol.* 2016;68(5):435–445. https://doi.org/10.1016/j.jacc.2016.05.057.
9. Kitabata H, Leipsic J, Patel MR, et al. Incidence and predictors of lesion-specific ischemia by FFR CT : learnings from the international ADVANCE registry. *J Cardiovasc Comput Tomogr.* 2018;12(2):95–100. https://doi.org/10.1016/j.jcct.2018.01.008.
10. Sand NPR, Veien KT, Nielsen SS, et al. PRrospEctive comparison of FFR derived from coronary CT angiography with SPECT PerfuSion imaging in stable coronary ArtEry DiSeaSe. *JACC Cardiovasc Imaging.* June 2018. https://doi.org/10.1016/j.jcmg.2018.05.004.
11. Fairbairn TA, Nieman K, Akasaka T, et al. Real-world clinical utility and impact on clinical decision-making of coronary computed tomography angiography-derived fractional flow reserve: lessons from the ADVANCE registry. *Eur Heart J.* August 2018. https://doi.org/10.1093/eurheartj/ehy530.
12. Kueh SH, Mooney J, Ohana M, et al. Fractional flow reserve derived from coronary computed tomography angiography reclassification rate using value distal to lesion compared to lowest value. *J Cardiovasc Comput Tomogr.* September 2017. https://doi.org/10.1016/j.jcct.2017.09.009.
13. Chinnaiyan KM, Akasaka T, Amano T, et al. Rationale, design and goals of the HeartFlow assessing diagnostic value of non-invasive FFRCT in Coronary Care (ADVANCE) registry. *J Cardiovasc Comput Tomogr.* December 2016. https://doi.org/10.1016/j.jcct.2016.12.002.
14. Agatston AS, Janowitz WR, Hildner FJ, Zusmer NR, Viamonte M, Detrano R. Quantification of coronary artery calcium using ultrafast computed tomography. *J Am Coll Cardiol.* 1990;15(4):827–832. https://doi.org/10.1016/0735-1097(90)90282-T.
15. Takagi H, Tanaka Ryoichi, Nagata Kyohei, et al. Diagnostic performance of coronary CT angiography with ultra-high-resolution CT: comparison with invasive coronary angiography. *Eur J Radiol.* 2018;101:30–37. https://doi.org/10.1016/j.ejrad.2018.01.030.
16. Abbara S, Arbab-Zadeh A, Callister TQ, et al. SCCT guidelines for performance of coronary computed tomographic angiography: a report of the society of cardiovascular computed tomography guidelines committee. *J Cardiovasc Comput Tomogr.* 2009;3(3):190–204. https://doi.org/10.1016/j.jcct.2009.03.004.
17. Abbara S, Blanke P, Maroules CD, et al. SCCT guidelines for the performance and acquisition of coronary computed tomographic angiography: a report of the society of cardiovascular computed tomography guidelines committee. *J Cardiovasc Comput Tomogr.* 2016;10(6):435–449. https://doi.org/10.1016/j.jcct.2016.10.002.
18. Hausleiter J, Meyer T, Hermann F, et al. Estimated radiation dose associated with cardiac CT angiography. *J Am Med Assoc.* 2009;301(5):500–507.
19. Leipsic J, Abbara S, Achenbach S, et al. SCCT guidelines for the interpretation and reporting of coronary CT angiography: a report of the society of cardiovascular computed tomography guidelines committee. *J Cardiovasc Comput Tomogr.* 2014;8(5):342–358. https://doi.org/10.1016/j.jcct.2014.07.003.
20. Youden WJ. Index for rating diagnostic tests. *Cancer.* 1950;3(1):32–35.
21. DeLong ER, DeLong DM, Clarke-Pearson DL. Comparing the areas under two or more correlated receiver operating characteristic curves: a nonparametric approach. *Biometrics.* 1988;44(3):837–845.
22. Dunn OJ. Multiple comparisons using rank sums. *Technometrics.* 1964;6(3):241–252. https://doi.org/10.2307/1266041.
23. Pencina MJ, D' Agostino RB, D' Agostino RB, Vasan RS. Evaluating the added predictive ability of a new marker: from area under the ROC curve to reclassification and beyond. *Stat Med.* 2008;27(2):157–172. https://doi.org/10.1002/sim.2929.
24. Cook NR, Paynter NP. Performance of reclassification statistics in comparing risk prediction models. *Biom J.* 2011;53(2):237–258. https://doi.org/10.1002/bimj.201000078.
25. Cury RC, Abbara S, Achenbach S, et al. CAD-RADSTM coronary artery disease – reporting and data system. An expert consensus document of the society of cardiovascular computed tomography (SCCT), the American college of Radiology (ACR) and the north American society for cardiovascular imaging (NASCI). endorsed by the American college of cardiology. *J Cardiovasc Comput Tomogr.* 2016;10(4):269–281. https://doi.org/10.1016/j.jcct.2016.04.005.